

Extreme Superheating and Supercooling of Encapsulated Metals in Fullerenelike Shells

F. Banhart,^{1,*} E. Hernández,² and M. Terrones³

¹Z. E. Elektronenmikroskopie, Universität Ulm, 89069 Ulm, Germany

²Institut de Ciència de Materials de Barcelona (ICMAB-CSIC), Campus de Bellaterra, 08193 Barcelona, Spain

³Advanced Materials Department, IPICYT, Venustiano Carranza 2425-A, Col. Lomas, 78210 San Luis Potosí, SLP México

(Received 11 December 2002; published 6 May 2003)

Nanometer-sized tin and lead crystals exhibit drastically altered melting and solidification behavior when encapsulated in fullerenelike graphitic shells. The melting transitions of encapsulated Sn and Pb nanocrystals are shown in an *in situ* electron microscopy study to occur at unexpectedly high temperatures, significantly higher than the melting point of the corresponding bulk materials. Atomistic simulations are used to show that the driving force for superheating is a pressure buildup of up to 3 GPa, that prevails inside graphitic shells under electron irradiation.

DOI: 10.1103/PhysRevLett.90.185502

PACS numbers: 61.46.+w, 61.48.+c, 64.70.Dv

There has been a long-standing uncertainty about the processes that lead to melting in solids [1,2]. Although the thermodynamics of melting and solidification predicts well-defined stability limits of the solid and liquid phases [3,4], the transformation is governed by nucleation kinetics [1,5,6]. Two criteria to account for the onset of melting have been frequently discussed in the literature. The first, known as Lindemann's criterion [7], stipulates that melting takes place once the thermal root mean squared displacement of atoms from their equilibrium positions in a crystal reaches a critical fraction of the nearest neighbor distance [typically (10–20)%]. The second, due to Born [8], states that melting occurs when the shear moduli of the crystal go to zero, i.e., the crystal loses its rigidity. Both criteria have been shown to be closely related in the recent work of Jin *et al.* [6]. In a freestanding crystal, melting starts at the surface, where the motion of atoms is less hindered, and thus the Lindemann criterion can be fulfilled at a lower temperature than elsewhere in the bulk. From there it propagates to the rest of the crystal, which eventually melts. Of particular interest is the melting behavior of nanometer-sized metal clusters [9] because these systems provide easier experimental access to the fundamental processes of melting. It is well known that free clusters melt below the melting temperature of the bulk, and that the difference between cluster and bulk melting temperatures usually scales as the inverse cubic root of the number of atoms in the cluster.

Superheating of a crystal (i.e., heating it up to a temperature above the equilibrium melting temperature) can be achieved by embedding it in a matrix of a higher melting point, if a sufficiently good lattice matching is possible at the interface between encapsulated crystal and confining matrix. Several examples of this have been reported in the literature [10–16]. If there is sufficient lattice matching at the interface, the motion of the encapsulated cluster atoms at the interface is hindered, and therefore they cannot serve as a melting nucleation site.

However, the role of other factors, such as pressure, should also be considered. In the existing literature on superheating of encapsulated clusters the role of pressure appears to be small [10,11]. In contrast, in this work we show that graphitic carbon onions can act as nanoscopic pressure cells in which encapsulated metal clusters exhibit very large superheating effects, even in the absence of a well-defined epitaxial interface.

The remarkable mechanical properties of carbon nanoparticles such as fullerenes, nanotubes, and carbon onions result from the extreme rigidity and strength of the covalent C-C bond in graphite [17,18]. In metal-graphite nanocomposites, these properties can be made use of in order to modify the morphology and physicochemical properties of metal nanocrystals [19]. In this study we report the experimental observation of drastic alterations in the melting and solidification behavior of nanoscale metal crystals that are encapsulated in fullerenelike graphitic shells. The melting temperatures of Sn and Pb crystals trapped inside graphite shells are significantly increased, much above the corresponding bulk melting temperatures. The opposite effect, i.e., the cooling of encapsulated liquid droplets below the bulk freezing point (supercooling) was also detected, though it was significant only in the case of Sn.

We have applied condensed-phase processes to produce graphitic cages containing metal crystals [20,21]. An electric current ($V = 20$ V; $I = 3$ – 5 A) was passed through graphite electrodes immersed in molten mixtures of LiCl/SnCl₂ (99:1 ratio) and LiCl/Pb (99:1 ratio) under an argon atmosphere at ca. 600–700 °C [22]. *In situ* electron microscopy studies of these materials were undertaken in a high-voltage transmission electron microscope (Jeol ARM-1250 at the Max Planck Institut für Metallforschung in Stuttgart) equipped with a heating specimen stage. The specimen temperature was varied between room temperature and 1100 K. Electron irradiation experiments were carried out with electrons of 1.25 MeV energy, and a beam intensity of approximately

100 A/cm². Electron energy-loss spectra (EELS) were recorded at each specimen temperature. Specimens consisting of partially encapsulated Sn and Pb crystals were irradiated at temperatures above 600 K using an intense electron beam in the electron microscope. By such treatment, metal nanocrystals within disordered graphitic material can be fully encapsulated in onion-like graphitic shells [23–25]. Indeed, graphitic shells were observed to wrap firmly around the metal crystals and form onion-like spherical particles with crystalline metal cores under electron irradiation. The encapsulated Sn and Pb cores were observed at different temperatures, and when melting of the metal core occurred, cooled down again. The crystallinity of the metal cores was verified by lattice imaging and by electron diffraction.

The encapsulated Sn crystals were found to be stable far above the bulk melting point of β -Sn ($T_m = 505$ K; the other known low-pressure phases of Sn have lower melting temperatures). Even at 770 K, solid crystals of Sn within graphitic shells were found, as shown in Fig. 1(a). Further observations were carried out at 920 and 1020 K, temperatures at which all Sn crystals (encapsulated or not) were molten. EELS spectra of the encapsulated Sn crystals showed no indication of an oxygen edge, thus excluding the presence of the metal oxide. To our knowledge, no stable Sn carbide exists, so the encapsulated material can be assumed to be essentially pure Sn. The encapsulated liquid Sn droplets were found to solidify well below the bulk melting temperature. As shown in Fig. 1(b), encapsulated Sn droplets persist in the liquid state down to 370 K.

As for Sn, superheating of encapsulated Pb crystals has also been observed in our experiments. Although the bulk melting temperature of Pb is 600 K, encapsulated Pb crystals were observed to be still in the solid state at

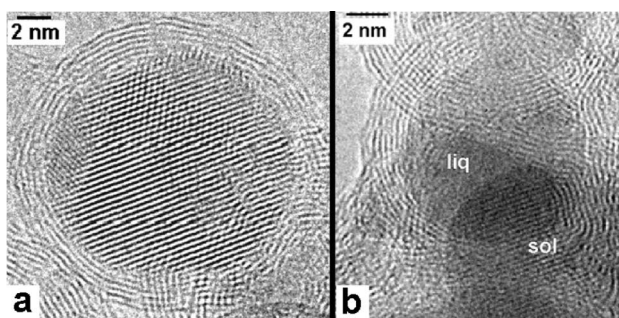


FIG. 1. Sn crystals encapsulated by graphitic onion-like shells. (a) Sn crystal (diameter 14 nm) superheated at 770 K. The lattice fringes of the core demonstrate the presence of Sn in the solid crystalline phase. The measured spacing of the fringes is 0.29 nm which corresponds to the (200) lattice planes of β -Sn. (b) Supercooled liquid Sn droplet (top, labeled “liq”) at 370 K. The specimen was subjected previously to high temperature so that melting occurred. A bare (not encapsulated) Sn particle (bottom, labeled “sol”) has already solidified. Several adjacent particles overlap in the projection.

740 K [see Fig. 2(a)]. However, at 870 K, all encapsulated Pb particles had molten, as can be seen in Fig. 2(b), indicating that the melting temperature of these superheated crystals occurred somewhere between these two temperatures. While the encapsulated Pb particles remained in the solid state, the lattice images were consistent with the projections of the fcc phase of Pb. Again, no trace of oxygen was found in the EELS spectra, and the formation of a Pb carbide can be excluded on the basis that no stable Pb carbide is known. However, one difference with the case of Sn was observed, namely, that upon cooling the sample, no significant supercooling of liquid Pb droplets was detected; rather, twins formed during or after the crystallization, possibly as a result of strain exerted by the encapsulating shells.

The hitherto reported superheating phenomena in confined environments are commonly rationalized in terms of the difference of solid-matrix and liquid-matrix interfacial energies [26]. If these energies are substantially different, as may occur when there is favorable epitaxy between solid cluster and matrix, then superheating can be appreciable. However, this explanation cannot account for the large superheating we find in our observations. This is because the c axis of the graphitic layers is normal to the interface around the whole particle; therefore no stable epitaxial interface is likely between the carbon layers and the confined metal core. In this particular case the driving force behind the observed superheating is an increase of pressure inside the carbon onions. The self-compression of carbon onions and the nucleation of diamond crystals in their cores under irradiation, as observed earlier [27], are a clear indication that irradiation leads to the buildup of high pressure at the cluster core. This occurs because irradiation with electrons of sufficient energy causes the sputtering of carbon atoms from the graphitic shells. Such a loss of atoms from the outer shells leads to a surface tension which results in a pressure buildup inside the carbon onions. Diffusion of the

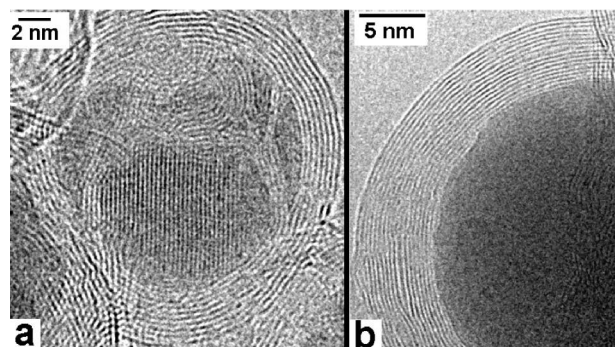


FIG. 2. Pb encapsulated by graphitic shells. (a) Crystalline Pb superheated at 740 K. The spacing of the lattice fringes is 0.29 nm, corresponding to the nominal spacing of the (111) planes (0.286 nm) in fcc crystals of Pb. (b) Liquid encapsulated Pb droplet (diameter ca. 30 nm) at 870 K.

encapsulated metal through the graphitic shells is possible, and indeed has been observed experimentally [23], but this process is too slow to counteract the buildup of pressure inside the metal cores. Therefore, a significant contribution to the observed superheating could be due to high pressures being exerted on the metal crystals by the graphitic shells. Up to the present, the magnitude of pressure inside carbon onions has not been directly accessible experimentally. In order to estimate the range of pressures exerted on the metal core, we have performed a series of atomistic simulations, focusing on the particular case of Pb.

We have used the empirical glue potential model due to Lim *et al.* [28], which has been used extensively to model Pb, and which accurately predicts the structure and melting temperature of Pb clusters. We have taken an fcc crystal consisting of 256 atoms in periodic boundary conditions (PBC) [29]. The use of PBCs eliminates the surface of the crystal, and emulates the effect of the encapsulation without having to explicitly consider the encapsulating object, i.e., the graphitic shells. We then performed isoshape isothermal-isobaric molecular dynamics simulations [30] at different temperatures and pressures. We started at 600 K (the bulk melting temperature of Pb) and raised the temperature up to 900 K in steps of 25 K, although when the melting transition was detected a smaller temperature interval was used to locate the transition more precisely. The pressures considered were 0, 0.5, 2.5, and 5 GPa. At each temperature and pressure simulations were carried out for times of 0.1 ns, using a time step of 10 fs, which proved to be sufficiently short to adequately conserve the total energy.

In Fig. 3 the volume per atom as a function of the temperature is shown for different pressures; melting transitions are manifested as discontinuities in the behavior of the volume. At zero pressure the system remains in the solid state up to $T \approx 690$ K, clearly above the thermodynamic melting temperature of the bulk (600 K), but well below the melting temperature in our experiments (between 740 and 860 K). This corresponds to the mechanical melting of an ideal Pb crystal without surfaces. The application of a small pressure (0.5 GPa) only raises the melting temperature by some 20 K. However, at 2.5 GPa, the crystal does not melt up to 860 K, approximately the temperature by which all encapsulated Pb clusters were experimentally observed to be in the liquid state. At a pressure of 5 GPa no melting was observed in the range of temperatures considered. These theoretical results allow us to estimate the range of pressures exerted on the metallic cores to be of the order of 2–3 GPa in our experiments, and confirm that high pressure prevails inside the graphitic shells under electron irradiation. It is also clear that such pressures do play a role in the large superheating effects observed in our experiments. The inset in Fig. 3 shows the mean squared displacements (MSD) averaged over all Pb atoms at 860 K (slightly

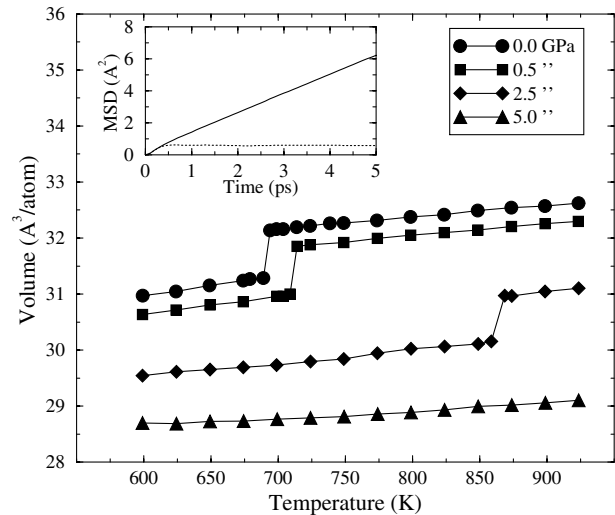


FIG. 3. Volume per atom as a function of temperature at different applied external pressures for Pb, as obtained from isoshape isothermal-isobaric simulations. The volume change at the melting transition is approximately 0.85 \AA^3 per atom in all three cases. The inset shows the mean-squared displacements (MSD) of the Pb atoms at a pressure of 2.5 GPa, and temperatures of 860 K (dotted line) and 870 K (solid line), i.e., just before and after the melting transition at this pressure. The flat MSD observed at 860 K results from thermal oscillations of the atoms around their equilibrium positions, indicating that the system is solid, while the finite slope of the solid curve at 870 K is typical of the diffusive behavior of the liquid state. From the slope of this curve a diffusion coefficient of $2.0 \times 10^{-5} \text{ cm}^2/\text{s}$ can be deduced.

below) and 870 K (slightly above) the detected melting transition at the pressure of 2.5 GPa. The magnitude of the MSD's just before melting has occurred gives an average thermal oscillation amplitude of approximately 0.7 \AA . Therefore, the root mean squared displacement of atoms from their equilibrium positions is approximately 0.35 \AA , which we identify as the critical displacement for melting at this pressure, according to the Lindemann criterion. It is surprising that this value is very similar in all cases where a melting transition was detected, independently of the temperature and pressure at which the melting transition occurred. This strongly suggests that the Lindemann critical value is the same along the solid-liquid coexistence curve, a point that deserves further investigation.

The observed supercooling of Sn can be explained [26] by the critical-sized stable grain that has to form for solidification to take place. The critical size depends on the temperature; the lower the temperature, the smaller the critical grain size. Solidification of encapsulated metals can therefore only occur once the temperature is low enough so that the critical-size solidification grain can be accommodated in the confined volume within the graphitic walls, and this probably explains the large supercooling effect observed in the case of Sn. The fact that a large

supercooling effect was not observed for Pb would imply that the critical nucleation grain required to solidify Pb is smaller than that of Sn. However, this issue warrants further study.

In conclusion, we have reported the experimental observation of large superheating effects in Sn and Pb clusters encapsulated in graphitic carbon onions. Supercooling was also observed, but was significant only in encapsulated Sn clusters. Since no well-defined epitaxial interface appears to occur at the carbon-metal interface, we believe that the usual explanation advocated in order to explain the superheating effect, namely, that there is a large difference between the matrix-solid and matrix-liquid interface energies, cannot fully account for the large superheating found in these systems. We argue that the pressure inside the carbon onions resulting from the electron bombardment in the electron microscope plays a major role in defining the extent of the observed superheating. We have carried out a thorough theoretical study using simulation techniques that allow us to establish that in the case of encapsulated Pb clusters the pressures required to account for the observed superheating are in the range of 2 to 3 GPa. The ability to encapsulate clusters of metals and possibly other materials inside carbon onions, combined with the possibility of exerting moderately large pressures on the encapsulates, opens a new avenue of research into the effects of pressure in the melting of materials at the nanoscale.

The authors are indebted to W. K. Hsu and N. Grobert for useful discussions and technical support in the preparation of the starting materials. We thank the MPI für Metallforschung in Stuttgart for giving us generous access to the electron microscopy facility. F. B. thanks the Deutsche Forschungsgemeinschaft, Sonderforschungsbereich 569, for financial support. E. H. thanks the Spanish Ministry of Science and Technology (MCyT) for supporting this work through Project No. BFM2002-03278. M. T. thanks the Alexander von Humboldt Stiftung (Germany) for support during the project, and also thanks CONACYT-México Grants No. W-8001-millennium initiative, No. 37589-U, No. G-25851-E, and the European Union Grant CNT-NET Project Contract No. G5RT-CT2001-05026 for financial support.

*Electronic address: Florian.Banhart@physik.uni-ulm.de

- [1] R. W. Cahn, *Nature (London)* **413**, 582 (2001).
- [2] J. G. Dash, *Rev. Mod. Phys.* **71**, 1737 (1999).
- [3] H. J. Fecht and W. L. Johnson, *Nature (London)* **334**, 50 (1988).
- [4] J. L. Tallon, *Nature (London)* **342**, 658 (1989).
- [5] R. W. Cahn, *Nature (London)* **323**, 668 (1986).
- [6] Z. H. Jin, P. Gumbsch, K. Lu, and E. Ma, *Phys. Rev. Lett.* **87**, 055703 (2001).
- [7] F. A. Lindemann, *Z. Phys.* **11**, 609 (1910).
- [8] M. Born, *J. Chem. Phys.* **7**, 591 (1939).
- [9] *Physics and Chemistry of Finite Systems: from Clusters to Crystals*, edited by P. Jena, S. N. Khanna, and B. K. Rao (Kluwer, Dordrecht, 1992).
- [10] C. J. Rossouw and S. E. Donnelly, *Phys. Rev. Lett.* **55**, 2960 (1985).
- [11] L. Gråbaek and J. Bohr, *Phys. Rev. Lett.* **64**, 934 (1990).
- [12] L. Gråbaek, J. Bohr, H. H. Andersen, A. Johansen, E. Johnson, L. Sarholt-Kristensen, and I. K. Robinson, *Phys. Rev. B* **45**, 2628 (1992).
- [13] S. Q. Xiao, S. Hinderberger, U. Dahmen, E. Johnson, A. Johansen, and K. K. Bourdelle, *J. Microsc.* **180**, 61 (1995).
- [14] H. W. Sheng, G. Ren, L. M. Peng, Z. Q. Hu, and K. Lu, *Philos. Mag. Lett.* **73**, 179 (1996).
- [15] R. Goswami and K. Chattopadhyay, *Philos. Mag. Lett.* **68**, 215 (1993).
- [16] H. Saka, Y. Nishikawa, and T. Imura, *Philos. Mag. A* **57**, 895 (1988).
- [17] M. S. Dresselhaus, G. Dresselhaus, and P. Eklund, *The Science of Fullerenes and Carbon Nanotubes* (Academic Press, New York, 1996).
- [18] P. J. F. Harris, *Carbon Nanotubes and Related Structures* (Cambridge University Press, Cambridge, United Kingdom, 1999).
- [19] F. Banhart, N. Grobert, M. Terrones, J.-C. Charlier, and P. M. Ajayan, *Int. J. Mod. Phys. B* **15**, 4037 (2001).
- [20] W. K. Hsu, J. P. Hare, M. Terrones, H. W. Kroto, D. R. M. Walton, and P. J. F. Harris, *Nature (London)* **377**, 687 (1995).
- [21] W. K. Hsu, H. Terrones, M. Terrones, N. Grobert, A. I. Kirkland, J. P. Hare, K. Prassides, P. D. Townsend, H. W. Kroto, and D. R. M. Walton, *Chem. Phys. Lett.* **284**, 177 (1998).
- [22] W. K. Hsu, J. Li, H. Terrones, M. Terrones, N. Grobert, Y. Q. Zhu, S. Trasobares, J. P. Hare, C. J. Pickett, H. W. Kroto, and D. R. M. Walton, *Chem. Phys. Lett.* **301**, 159 (1999).
- [23] F. Banhart, P. Redlich, and P. M. Ajayan, *Chem. Phys. Lett.* **292**, 554 (1998).
- [24] F. Banhart, *Rep. Prog. Phys.* **62**, 1181 (1999).
- [25] F. Banhart, J.-C. Charlier, and P. M. Ajayan, *Phys. Rev. Lett.* **84**, 686 (2000).
- [26] H. K. Christenson, *J. Phys. Condens. Matter* **13**, R95 (2001).
- [27] F. Banhart and P. M. Ajayan, *Nature (London)* **382**, 433 (1996).
- [28] H. S. Lim, C. K. Ong, and F. Ercolessi, *Surf. Sci.* **269/270**, 1109 (1992); H. S. Lim, C. K. Ong, and F. Ercolessi, *Z. Phys. D* **26**, S45 (1993).
- [29] M. P. Allen and D. J. Tildesley, *Computer Simulation of Liquids* (Clarendon Press, Oxford, 1987).
- [30] E. Hernández, *J. Chem. Phys.* **115**, 10 282 (2001); *Comput. Mater. Sci.* **27**, 212 (2003).